Journal of Engineering and Technology for Industrial Applications

ISSN ONLINE: 2447-0228

ITEGAM-JETIA

Manaus, v.11 n.54, p. 140-146. July/August., 2025.

DOI: https://doi.org/10.5935/jetia. v11i54.2338

RESEARCH ARTICLE OPEN ACCESS

COMPUTATIONAL THERMAL ANALYSIS OF FeCrV15+TiB_2 COATINGS ON EN48 BASEPLATE BY USING THE COMSOL MULTIPHYSICS

Basiru Philip Aramide [1], Tamba Jamiru [2], Taoreed Adesola Adegbola [3], Abimbola Patricia Idowu Popoola [4], Mathew Olurotimi Adeoti [5], Rotimi Sadiku [6] and Sisa Pityana [7]

[1, 2. 3, 5] Department of Mechanical and Mechatronics Engineering, Tshwane University of Technology, Pretoria South Africa

[4, 6] Department of Chemical, Metallurgical & Material Engineering, Tshwane University Technology, Pretoria, South Africa

[7] National Laser Centre, Council for Scientific and Industrial Research, Pretoria

[1] http://orcid.org/0000-0002-6488-1287, [2]http://orcid.org/0000-0002-9492-1921, [3]http://orcid.org/0000-0002-6881-7215, [4]http://orcid.org/0000-0003-4447-8551, [5]http://orcid.org/0009-0006-9308-0936, [6]http://orcid.org/0000-0002-8504-1041, [7]http://orcid.org/0000-0002-9273-2043,

Email: abashiruphilip@gmail.com, JamiruT@tut.ac.za, AdesolaAT@tut.ac.za, PopoolaAPI@tut.ac.za, AdeotiMO@tut.ac.za, SadikuR@tut.ac.za, SPityana@csir.co.za.

ARTICLE INFO

Article History
Received: July 9, 2025
Revised: July 13, 2025
Accepted: June 15, 2025
Published: July 31, 2025

Keywords:
Laser cladding,
Laser irradiation,
Additive Manufacturing,
3D simulation,
Modelling.

ABSTRACT

This study seeks to elucidate the thermal effects of including TiB2 powder on the geometric evolution of FeCrV15 coating using a 3D simulation of the laser cladding process. The process entails applying a coating of FeCrV15 powder onto the EN48 substrate and incorporating TiB2 powder into the coating to evaluate the feasibility of IPG laser-applied coating layers. In order to modify the laser cladding process, the conservation equations of energy, momentum, and mass are linked via the temperature variable and resolved. Intricate hypotheses are employed in mathematical modeling to address the boundary conditions arising from the laser melting of several materials, thereby simplifying issues associated with varying material properties. Moving mesh is employed to ascertain the deformation of a free surface by utilizing the Arbitrary Lagrangian and Eulerian (ALE) methodology. The simulation disregards thermo-capillary forces and their influence on fluid dynamics within the liquefied pool to achieve process optimization. The developed procedure simulation also assesses the thermal dispersion associated with the procedure. The results provide approximate information regarding the influence of TiB2 on the development of clad geometry and the thermal gradient.

I. INTRODUCTION

The laser cladding process stands out as a promising additive manufacturing (AM) technique for depositing thick layers onto both similar and dissimilar coatings, particularly those of considerable thickness. The advancement of laser-based systems for powder deposition onto substrates has garnered significant attention across various industrial applications, particularly in thick cladding, coatings, and repair processes [1], [2]. Metal additive manufacturing holds significant promise across various industries because of its capacity to fabricate intricate shapes that conventional methods cannot achieve. This capability not only enhances performance but also contributes to cost reduction and accelerates development timelines. Industries such as aerospace and medical, where the demand for customized and intricate parts is prevalent, find metal additive manufacturing particularly beneficial. Moreover, this technology proves to be practical for high-mix low-volume production scenarios, which are frequently encountered in these sectors [2-5]. However, optimising this process poses several critical challenges, including achieving the desired properties for the final cladding layer such as uniform thickness, strong bonding, and minimizing dissolution and deformations [6], [7]. The experimental setup presents several constraints owing to intricate technical hurdles. Factors such as laser power selection, laser beam spot size, laser travel speed, shield gas flow, powder feed rate, and surface preparations significantly impact the end product's quality in the manufacturing process [8], [9].

Laser cladding made its debut in the early 1980s, quickly becoming a staple in industrial coating and repair processes. Over time, it evolved into a method for additive manufacturing of entire 3D parts. Today, its applications continue to expand, encompassing various industries, including additive manufacturing. As this field progresses, simulation becomes increasingly vital, offering valuable predictive capabilities to further advance laser cladding technologies [10], [11]. Numerous publications in the literature explore numerical simulations of the laser cladding process, unveiling a multitude of effective methodologies. However, according to Wirth and Wegener [11], upon examination of selected exemplary publications, it becomes evident that each model exhibits certain limitations. These shortcomings typically revolve around issues such as the treatment of free surfaces, the accuracy of heat source modelling, and the incorporation of subprocess models like powder jet models. However, the extent of these shortcomings has not been quantified. Wirth and Wegener [11] introduced a comprehensive, physics-driven integrated model. They aimed to amalgamate the most effective methodologies from existing literature to enhance predictive capabilities and enable simulation-based insights for deeper process comprehension. They sought to assess the ramifications and boundaries of model simplification, which can be nontrivial. This integrated model spans from simulating powder particle flow, through melt pool dynamics, to structural and material simulations, hence earning the designation of "integrated".

The powder particle flow simulation and the melt pool region model was previously documented Wirth et al. and Wirth and Wegener respectively [11], [12]. Pinkerton [13] underscores in his review paper on laser cladding modeling the promising prospect for notably enhanced models, particularly through the integration of sub-process models. Moreover, Manvatkar et al. [14] assert the absence of a computationally efficient 3D laser cladding process model encompassing heat transfer, powder addition, build geometry, and thermal cycles in multilayer laser additive manufacturing processes. In this text, the thermal impact of introducing TiB_2 powder into *FeCrV15* coating model is outlined. The properties of *FeCrV15* alloy are presented in **Table 1**.

Table 1: Properties of *FeCrV15* alloy powder.

Property	**Value**
Coefficient of thermal expansion	3.79e-6[1/K]
Heat capacity at constant pressure	483.88 [J/(kg*K)]
Density	7204.14[kg/m^3]
Thermal conductivity	76.718[W/(m*K)]
Young's modulus	201e9[Pa]
Poisson's ratio	0.29

Source: Authors, (2025).

II. MATHEMATICAL FRAMEWORK

The procedures encompassed with laser cladding, like liquifying and solidifying cycles, are comparable to welding phenomena, where as a consequence, modelling the laser beam heating and mass addition proves difficult. The boundary conditions must be appropriately dispersed by having the material properties and the procedure parameters in mind during the heating process. The attained set of model equations, combined with the temperature variable have undergone mathematical treatment, and they have been resolved through the COMSOL multi-physics software. For reference, see **Figure 1** for a representation of the laser cladding process phenomenon and laser beam interaction characteristics. Through the use of Arbitrary Lagrangian and Eulerian (ALE) equations, deformed geometry is brought about by continual heating and mass addition [15].

II.1 POSTULATIONS

- The powder grains are assumed to be sphere-like objects with a radius r_p.
- The thickness of the liquified pool is assumed to be equivalent to the thickness of the laser beam, and the shape of the liquid pool is assumed to have an oval-shaped cross-section.
- During the model's formulation, the material loss caused by evaporation is not taken into account.
- Throughout the process, the energy stored by the powder grains and the steel substrate material stays uniform and unchanging.
- Due to the short duration of the powder particles' interaction with the laser, there is no loss of heat by either radiation or convection by the powder grains.
- Less than 2% of the energy received by the substrate is made up of the energy admitted by the powder grains.
- Since liquid metal and air have such a large viscosity and density difference, we may decrease zone calculation without taking the air into account.
- The Newtonian fluid that makes up the liquid metal is considered incompressible, and Laminar flow is assumed to be present in the molten pool [15].

II.2 ZONES' GOVERNING EQUATIONS

At first, the issue is formulated by assuming that the laser beam heat flux covers the steel plate region's laser beam interaction surface (Gaussian). In Zone A, the predominant phenomenon is the heat conduction process (as shown in **Figure 1**). The residual *FeCrV15* powder that was laser-melted and a small area of the *EN48* steel melt pool is also depicted in Zone B. Mass and momentum conservation have now replaced the energy conservation phenomenon [15].

II.2.1 Energy Conservation

$$\rho C_\rho \frac{\partial T}{\partial t} + \rho C_\rho \boldsymbol{u} \cdot \nabla T + \nabla \cdot \boldsymbol{q} = Q + Qted \tag{1}$$

$$\boldsymbol{q} = -k\nabla T \tag{2}$$

ρ is the density, C_ρ is specific heat capacity, T is temperature, k is thermal conductivity
$Q + Q_{ted}$ is power generation per unit volume of the substrate Q_v.

The momentum and mass conservation equations were used to determine the velocity field u in the equation above.

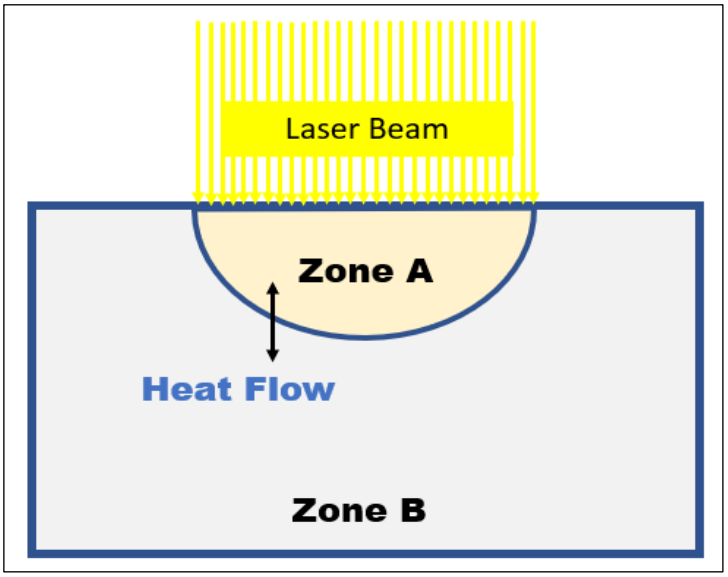

Figure 1: Process phenomena in Physics.
Source: Authors, (2025).

II.2.2 Conservation of Momentum

One of the key controlling laws in the laser cladding process is the conservation of momentum. The representation of the momentum equation is

$$\rho_0 \left[\frac{\partial u}{\partial T} + u(\nabla u)\right] = \nabla[-pI + \mu(\nabla u + (\nabla u)^T] + F_b + F_G \quad (3)$$

Where ρ_0 is the density at $T = T_m$, F_b is Buoyancy Force, F_G is Darcy Force.

II.2.3 Mass Conservation

The continuity equation is depicted as follows:

$$\nabla u = 0 \quad (4)$$

As the specific heat capacity rises, the impact of latent heat of fusion on the temperature distribution can be roughly estimated, thus:

$$C_p = C_p + \Delta H_m \frac{\partial L_f}{\partial T} \quad (5)$$

ΔH_m is the latent heat of fusion, L_f is liquid fraction

The following equation incorporates buoyancy force into the momentum equation:

$$F_b = \rho_0[1 - \beta(T - T_o)]g \quad (6)$$

β is thermal expansion co-efficient, g is gravity field

The Darcy's governing equation for the momentum equation, is given by

$$F_G = \frac{-180\mu}{d^2}\frac{(1-L_f)^2}{({L_f}^3+\tau)}u \quad (7)$$

τ is a numerical constant, d is powder diameter, μ is viscusity

Liquid fraction L_f can be expressed as follows:

$$L_f = \begin{cases} 0 & T_s \leq T \\ \frac{T-T_s}{T_L-T_s} & T_s < T < T_L \\ 1 & T > T_L \end{cases} \quad (8)$$

II.3 BOUNDARY CONDITIONS

A number of challenging boundary criteria must be met for the laser cladding simulation procedure. However, the following list of the necessary boundary conditions is provided:

- By using a surface heat source and heat flux determined by the boundary condition, on the impact of the laser beam and the flux of powder, may be simulated.

$$q_{in} = \propto_0 \cos(\theta) I_0 - h_c(T - T_o) - \varepsilon_t \sigma\left(T^4 - {T_o}^4\right) \text{(For Zone A)} \quad (9)$$

$$q_{in} = -h_c(T - T_o) - \varepsilon_t \sigma\left(T^4 - {T_o}^4\right) \text{ (For Zone B)} \quad (10)$$

h_c is heat convection coefficient, $\propto_0$ is absorption factor, ε_t is emissivity, σ is Stefan-Boltzmann constant.

- For energy distribution, a continuous laser beam of uniform intensity is taken into consideration. The following formula was used to calculate the laser beam's intensity.

$$I_0 = Laser\ intensity = \begin{matrix} \frac{\propto_0 \cos\theta P_l}{\pi r^2} & r \le r_l \\ 0 & r > r_l \end{matrix} \quad (11)$$

P_l is laser average power, r_l is beam radius

II.3.1 Boundary Conditions for Fluid Flow

The thermocapillary and melt pool capillary forces act in the normal and tangential directions on the free surface. The appropriate force equations are shown below:

$$\sigma_n = -p_\propto \vec{n} Y(T) \kappa \vec{n} \text{ (For Zone A)} \quad (12)$$

$$\sigma_t = \frac{\partial Y}{\partial T} \nabla T \vec{t} \text{ (For Zone A)} \quad (13)$$

$$u = 0 \text{ (For Zone B)} \quad (14)$$

$p_\propto$ is ambient pressure, $\vec{n}$ is normal vector of the free surface, κ is curvature, $\vec{t}$ is tangential vector to the free surface, Y is surface tension

II.3.2 Moving Mesh

A liquid/solid boundary and a liquid/gas boundary are moving interfaces in the finite element model. An ALE approach is used to track overtly, only the liquid/gas contact. In this method, zone nodes obey a nearly Eulerian account, while border nodes are governed by fluid mechanics processes and insured by a Lagrangian account (see **Figure 2**). However, internal nodes are shifted to prevent numerical instability when computing. Winslow and Laplace are two smoothing techniques that COMSOL Multi-Physics suggests to regulate the node displacement. The Winslow method is used to make the computations provided, an expression is used to connect the ALE method with the conservation and momentum equations [15].

$$V_{mesh}\vec{n} = V_{mat}\vec{n} \text{ (For Zone A)} \quad (15)$$

$$V\vec{n} = 0 \text{ (For Zone B)} \quad (16)$$

V_{mesh} is the mesh speed (m/s), and V_{mat} stands for the calculated material velocity (m/s) using momentum conservation equations.

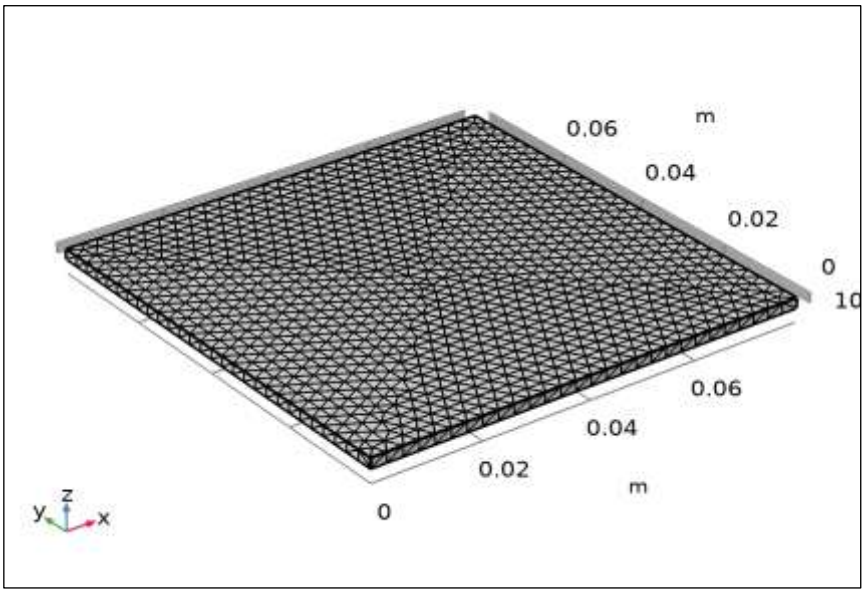

Figure 2: The Moving Mesh.
Source: Authors, (2025).

III. MATERIALS AND METHODS

To analyse the impact of introducing TiB_2 powder on the clad geometry, a computational model was built, centering on the positions of laser power entering and exiting from the heated pool. By including all mathematical equations in a 3D model, COMSOL Multi-Physics was employed to run a series of finite element modelling (FEM) simulations. This technique's first step is to define the process globally (global definition), taking advantage of all possibilities, such as input procedure parameters, variables, functions, and geometry subsequences, required in the problem definition. Three separate branches of physics—heat transfer, structural mechanics, and mathematics—are incorporated into the model for the laser cladding simulation technique. However, this section is limited to the report on how the introduction of TiB_2 powder affects the heat transfer, which invariably affects the clad geometry [15]. The initial rectangular cuboid created during model development has a steel substrate's length, breadth, and thickness (see **Figure 3**).

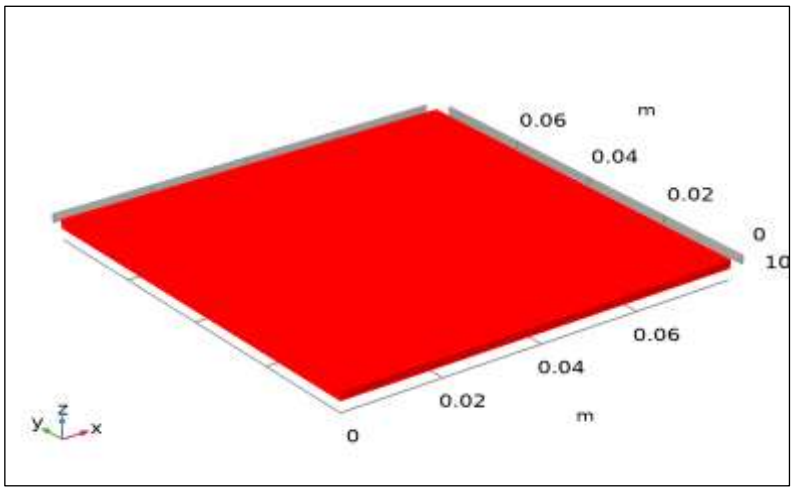

Figure 3: The rectangular cuboid steel substrate.
Source: Authors, (2025).

The ellipse is built individually to represent the clad geometry and makes the geometry whole by Boolean operations. The beam size variation changes the clad dimension because the elliptical size is connected to the laser beam diameters. Triangular elements are utilised in the meshing procedure for 3D modelling of the laser cladding process (see **Figure 2**). In COMSOL Multi-Physics, the Winslow approach is used to generate deformed meshes as a result of moving heat sources. The cladding process's linked thermomechanical analysis is predicated on the idea that the temperature field from the thermal exploration functions as the foundation for predictions of the clad's shape and dilution. In order to examine the influence of the TiB_2 introduction on the final geometry of the coatings, the input procedure parameters in the simulation models are based on experimental procedure prerequisites.

IV. RESULTS AND DISCUSSIONS

The results of the simulation and the experimental coatings are presented in **Figure 4**. The coatings of *FeCrV15* show smooth, perfectly, and metallurgically bounded deposits on EN48 steel substrate (see **Figures 4a** & **c**), whereas the coating became rough with cracks and pores upon introducing TiB_2 powder at the same laser parameters (see **Figures 4b** & **d**). An endothermic reaction was observed when TiB_2 was introduced during the experimentation. Both coatings' thermal stress distributions are represented in **Figure 5**. The thermal stress distribution of *FeCrV15*+TiB_2 coating is 477 K, far higher than *FeCrV15* coating, which is 366 K, which may be responsible for the observed pores and cracks in the *FeCrV15*+TiB_2 coating.

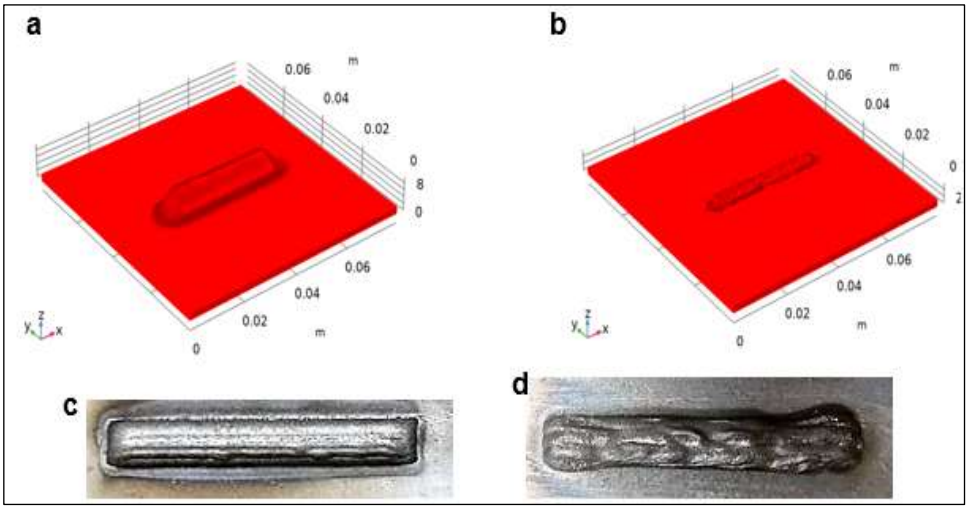

Figure 4: Modelled coated samples (a) & (c) *FeCrV15* coating and (b) & (d) *FeCrV15*+TiB_2 coating.
Source: Authors, (2025).

This implies that introducing TiB_2 powder into *FeCrV15* coating resulted in increasing the thermal input, which increases the stress within the deposit, creating the cracks and pores as observed in **Figure 6.**

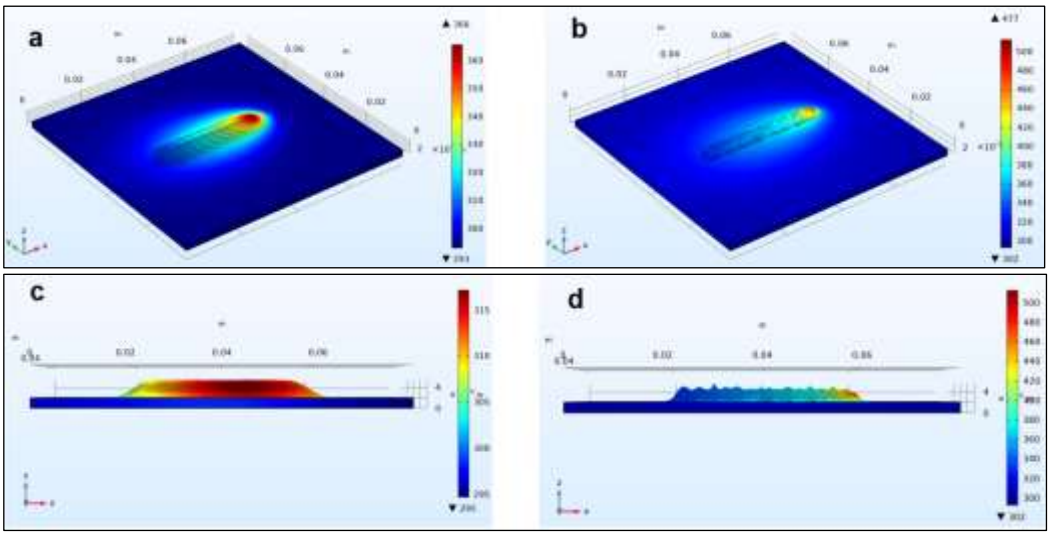

Figure 5: Thermal stress distribution of the deposited coatings (a) & (c) *FeCrV15* coating and (b) & (d) *FeCrV15+TiB₂* coating.
Source: Authors, (2025).

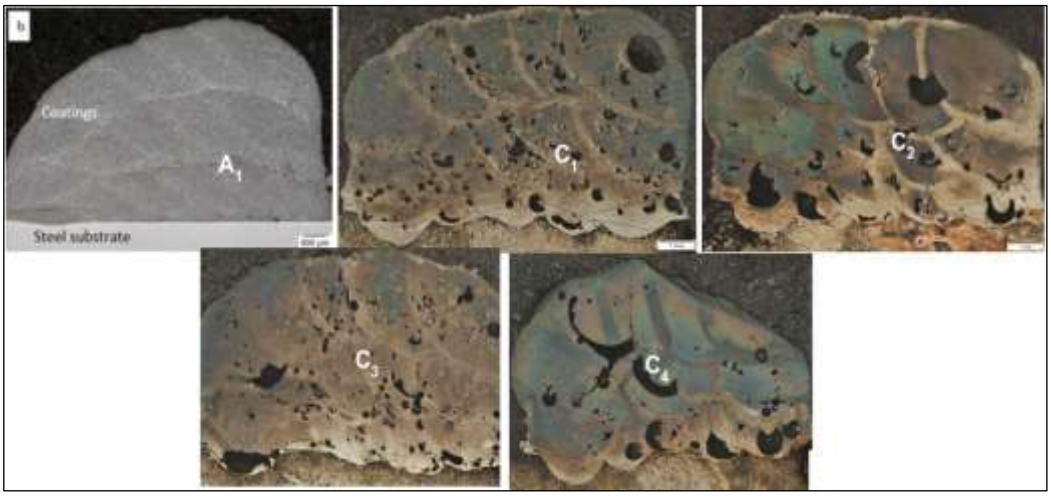

Figure 6: Optical microscope of *FeCrV15* (A_1) coating and *FeCrV15+TiB₂* (C_1, C_2, C_3, & C_4) coatings.
Source: [16]

V. CONCLUSIONS

In conclusion, this study delves into the thermal implications of incorporating TiB2 powder into FeCrV15 coating via 3D laser cladding simulation. By linking conservation equations of energy, momentum, and mass and utilizing complex mathematical modeling, the research sheds light on clad geometry development and thermal gradients. Although thermo-capillary forces are neglected, the simulation effectively evaluates process-related thermal distributions. Results demonstrate that introducing TiB2 alters clad geometry and thermal stress distribution, as evidenced by the roughness, cracks, and pores observed in coated samples. The significant increase in thermal stress in TiB2-modified coatings suggests heightened thermal input, contributing to defect formation. This research underscores the importance of simulation in enhancing understanding and optimization of laser cladding processes, offering valuable insights for industrial applications in aerospace, automotive, and tooling sectors.

VI. AUTHOR'S CONTRIBUTION

Conceptualization: Basiru Philip Aramide and Sisa Pityana..
Methodology: Basiru Philip Aramide and Sisa Pityana.
Investigation: Basiru Philip Aramide and Mathew O. Adeoti
Discussion of results: Basiru Philip Aramide, Taoreed Adesola Adegbolam and Tamba Jamiru.
Writing – Original Draft: Basiru Philip Aramide.
Writing – Review and Editing: Basiru Philip Aramide and Rotimi Sadiku.
Resources: Patricia Popoola, Rotimi Sadiku, Tamba Jamiru and Sisa Pityana
Supervision: Patricia Popoola, Rotimi Sadiku, Tamba Jamiru and Sisa Pityana
Approval of the final text: All authors

VII. ACKNOWLEDGMENTS

The authors acknowledge the financial support from Tshwane University of Technology (TUT), Pretoria, South Africa, without which this work would not have been possible.

VIII. REFERENCES

[1] J. Mazumder, D. Dutta, N. Kikuchi, and A. Ghosh, "Closed loop direct metal deposition: art to part," Optics and Lasers in Engineering, vol. 34, no. 4-6, pp. 397-414, 2000.

[2] Y. Kuroiwa, D. Kono, and Y. Oda, "INVESTIGATION ON THERMAL DEFORMATION IN LASER ADDITIVE MANUFACTURING," MM Science Journal, 2021.

[3] P. Bartolo et al., "Biomedical production of implants by additive electro-chemical and physical processes," CIRP annals, vol. 61, no. 2, pp. 635-655, 2012.

[4] M. K. Thompson et al., "Design for Additive Manufacturing: Trends, opportunities, considerations, and constraints," CIRP annals, vol. 65, no. 2, pp. 737-760, 2016.

[5] F. Klocke et al., "Turbomachinery component manufacture by application of electrochemical, electro-physical and photonic processes," CIRP annals, vol. 63, no. 2, pp. 703-726, 2014.

[6] E. Amara, L. Achab, and O. Boumia, "Numerical modelling of the laser cladding process using a dynamic mesh approach," in Proceedings of CAOL 2005. Second International Conference on Advanced Optoelectronics and Lasers, 2005., 2005, vol. 1: IEEE, pp. 142-145.

[7] J. Hofman, D. De Lange, B. Pathiraj, and J. Meijer, "FEM modeling and experimental verification for dilution control in laser cladding," Journal of Materials Processing Technology, vol. 211, no. 2, pp. 187-196, 2011.

[8] S. Tsirkas, P. Papanikos, and T. Kermanidis, "Numerical simulation of the laser welding process in butt-joint specimens," Journal of materials processing technology, vol. 134, no. 1, pp. 59-69, 2003.

[9] H.-y. Zhao, H.-t. Zhang, C.-h. Xu, and X.-Q. Yang, "Temperature and stress fields of multi-track laser cladding," Transactions of Nonferrous Metals Society of China, vol. 19, pp. s495-s501, 2009.

[10] A. Weisheit, A. Gasser, G. Backes, T. Jambor, N. Pirch, and K. Wissenbach, "Direct Laser Cladding, Current Status and Future Scope of Application," in Laser-Assisted Fabrication of Materials, J. D. Majumdar and I. Manna Eds. Berlin, Heidelberg: Springer Berlin Heidelberg, 2013, pp. 221-240.

[11] F. Wirth and K. Wegener, "A physical modeling and predictive simulation of the laser cladding process," Additive Manufacturing, vol. 22, pp. 307-319, 2018/08/01/ 2018, doi: https://doi.org/10.1016/j.addma.2018.05.017.

[12] F. Wirth, S. Freihse, D. Eisenbarth, and K. Wegener, "Interaction of powder jet and laser beam in blown powder laser deposition processes: measurement and simulation methods," in Lasers in Manufacturing Conference, Munich, Germany, 2017, pp. 1-10.

[13] A. J. Pinkerton, "Advances in the modeling of laser direct metal deposition," Journal of Laser Applications, vol. 27, no. S1, 2014, doi: 10.2351/1.4815992.

[14] V. Manvatkar, A. De, and T. DebRoy, "Spatial variation of melt pool geometry, peak temperature and solidification parameters during laser assisted additive manufacturing process," Materials Science and Technology (United Kingdom), Article vol. 31, no. 8, pp. 924-930, 2015, doi: 10.1179/1743284714Y.0000000701.

[15] R. Parekh, R. K. Buddu, and R. Patel, "Multiphysics simulation of laser cladding process to study the effect of process parameters on clad geometry," Procedia Technology, vol. 23, pp. 529-536, 2016.

[16] B. P. Aramide, T. Jamiru, T. A. Adegbola, A. P. I. Popoola, and E. R. Sadiku, "Influence of TiB2 Incorporation on Microstructural Evolution in Laser-Clad FeCrV15 + TiB2 Deposits," Journal of Materials Engineering and Performance, 2024/05/23 2024, doi: 10.1007/s11665-024-09618-w.